

# Microstructural changes in Oxisols under long-term different management systems

Aristides Osvaldo Ngolo<sup>(1)</sup> , Fábio Soares de Oliveira<sup>(2)</sup> , Maurílio Fernandes de Oliveira<sup>(3)</sup>  and Raphael Bragança Alves Fernandes<sup>(4)\*</sup> 

<sup>(1)</sup> Centro Nacional de Investigação Científica, Luanda, Angola.

<sup>(2)</sup> Universidade Federal de Minas Gerais, Instituto de Geociências, Departamento de Geografia, Belo Horizonte, Minas Gerais, Brasil.

<sup>(3)</sup> Empresa Brasileira de Pesquisa Agropecuária, Embrapa Milho e Sorgo, Sete Lagoas, Minas Gerais, Brasil.

<sup>(4)</sup> Universidade Federal de Viçosa, Departamento de Solos, Viçosa, Minas Gerais, Brasil.

**ABSTRACT:** There has long been a discussion about the effects of soil management on its structure. Since changes can occur due to management and time of use, more accurate assessments can be achieved if carried out in long-term experiments. This study investigated the long-term effects of soil management on the physical quality of a Cerrado Oxisol (Latosolo Vermelho), focusing on microstructural changes. Micromorphology and computed tomography techniques were used to assess the soil's microstructure. The study compared areas under long-term and different soil management practices, including disc plowing, no-tillage, and disc harrow+subsoiler. A native Cerrado area was considered as the reference. Micromorphology revealed some changes in the pedological features of soil aggregates, but the granular structure showed good resistance even after two decades of use and management. It also indicated a decrease in larger pores and an increase in the surface soil layer micropores for the disc plowing and no-tillage treatments. These results were consistent with traditional laboratory evaluations of soil porosity. Computed tomography was limited due to increased soil bulk density in the cultivated treatments, but it showed potential for assessing soil porosity and pore connectivity. We concluded that micromorphology effectively identifies microstructural changes in Oxisols with small and strong granular structures, and the granular soil aggregates displayed resilience even after long-term management. The micromorphometric evaluation corroborates with traditional methods and suggests loss of pores associated with the disc harrow+subsoiler treatment.

**Keywords:** soil microstructure, pores morphometry, X-ray microtomography, soil micromorphology.

\* **Corresponding author:**  
E-mail: raphael@ufv.br

**Received:** May 16, 2023

**Approved:** August 03, 2023

**How to cite:** Ngolo AO, Oliveira FS, Oliveira MF, Fernandes RBA. Microstructural changes in Oxisols under long-term different management systems. Rev Bras Cienc Solo. 2023;47:e0230051. <https://doi.org/10.36783/18069657rbcs20230051>

**Editors:** José Miguel Reichert  and Edivan Rodrigues de Souza 

**Copyright:** This is an open-access article distributed under the terms of the Creative Commons Attribution License, which permits unrestricted use, distribution, and reproduction in any medium, provided that the original author and source are credited.



## INTRODUCTION

Soil structure maintenance is a key factor to guarantee the proper functioning of the physical, chemical, and biological soil properties, contributing to establishing more resilient and sustainable productive systems. Traditionally, the soil structure has been understood as the set of particles of different shapes and sizes, its distribution and arrangement, in which the soil can be disintegrated, giving rise to different aggregates (Tang et al., 2023; Yudina and Kuzyakov, 2023).

The concept of soil structure in natural systems includes complex interactions among biological activity, soil minerals, and local climate, which promote the aggregation and accumulation of biopores (Or et al., 2021). This important complex physical property is influenced by different physical-chemical and biological factors but is also primarily dependent on the five factors of soil formation (parent material, climate, vegetation, topography, time). Nevertheless, the cultivation models adopted for long years, based on soil tillage with plows and harrows, have negatively impacted soil structure, reducing soil quality.

To understand the effects on soil macrostructure, a deep understanding of its microstructure evolution is first required (Tang et al., 2023). Understanding microstructural characteristics such as pore architecture and orientation, the arrangement and distribution of aggregates are fundamental to ensuring the proper functioning of the soil-plant system. Good soil structure and other soil attributes, such as high aggregate stability, are essential for supporting important functions such as biomass production, soil fertility, water, and carbon storage (Meurer et al., 2020). However, as a result of soil management, changes can occur in aggregate microstructure, such as pore size, shape, distribution, and pore connectivity, which directly affect soil water infiltration and retention (Fichtner et al., 2019), as well as the movement and storage of nutrients (Lawrence and Jiang, 2017).

Several methods have been used to assess the soil microstructure, including X-ray computed tomography (CT), synchrotron-based microanalyses, field emission scanning electron microscope, scanning electron microscopy, mercury intrusion porosimetry, laser particle size analysis (Malobane et al., 2021; Shen et al., 2022; Gerzabek et al., 2023; Jiang et al., 2023; Ye et al., 2023). This study applied photomicrography and CT techniques to assess the effects of long-term management on soil physical properties. The hypothesis is that long-term conventional cultivation practices and no-tillage may lead to modifications in soil microstructure, even for those with a well-developed granular structure.

Photomicrographs allow assessing porous soil space based on qualitative and quantitative studies, identifying patterns related to forming pores and, consequently, their transformation under management (Ferreira et al., 2018). Because of the interest in contributing to understanding interventions that can lead to soil degradation, this study aimed to evaluate the long-term micromorphological transformations resulting from different soil management in a *Latossolo Vermelho* (Oxisol) under Cerrado (Brazilian Savanna).

## MATERIALS AND METHODS

### Soil sampling and long-term soil management types

The study was carried out on a typical *Latossolo Vermelho Distrófico* (dRL), according to the Brazilian Soil Classification System (Santos et al., 2018). This soil class corresponds to Oxisols (Soil Taxonomy) and Ferralsols (WRB/FAO). This soil is associated with limestones of the Sete Lagoas Formation, Bambuí Super Group, a Neoproterozoic lithostratigraphic unit (Costa and Branco, 1961) composed by a succession of carbonate rocks and metapelites settling directly on the granite-gneiss basement (Brandalise et al., 1980). These Oxisols are generally under flat to smooth undulating relief, facilitating intensive agricultural use.

We developed this study on an experimental unit of Embrapa Milho e Sorgo, in the municipality of Sete Lagoas (Minas Gerais State - Brazil), central coordinates 19° 27.408' S and 44° 10.939' W, and 786 m a.s.l (Figure 1). The prevailing region climate is Cwa, according to Köppen classification system, characterized by having dry winter and hot summer, with a warmer month temperature above 22 °C.

The historical soil use in the experimental area is presented in table 1. The experiment was installed in 1995 with corn plantations under different soil management types. Until the soil samples collection (2016), the experimental area was cultivated in plots (20 × 20 m), with 11 treatments distributed in randomized blocks. We selected three soil management types for this study: disc plowing (DP), no-tillage (NT), and disc harrowing+subsoiler (DHS). We selected for control and comparison purposes the Oxisol under Native Cerrado (NC). All treatments, including the Native Cerrado (NC), occur on the same slope, landscape position, and exposure face to solar radiation.

### Analyses

Soil trenches were opened in each experimental plot for soil micromorphology analyses and, using cardboard boxes (15 × 10 cm), undisturbed soil samples were collected from the layers corresponding to Surface (0.00-0.05 m), A Horizon (0.10-0.15 m) and Bw Horizon (0.50-0.55 m). From each of the four treatments, an experimental plot was chosen where the samples in duplicate were taken, thus corresponding to a total of 24 samples.

Micromorphological analyses were carried out in undisturbed soil samples collected in the NC, DP, DHS, and NT management types at 0.00-0.05 m (Surface), 0.10-0.15 m (A horizon), and 0.50-0.55 m (B horizon) depths. The samples were vacuum-impregnated

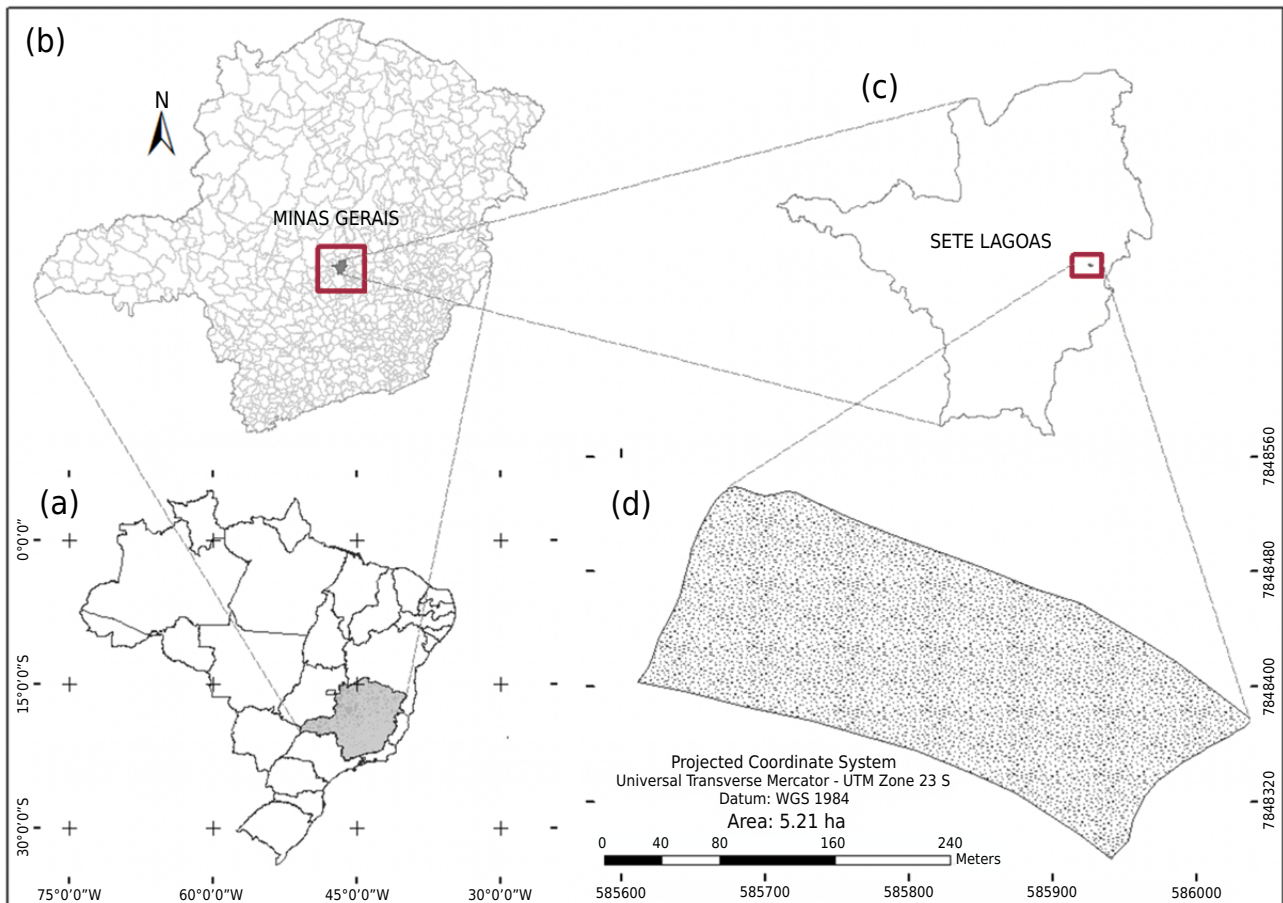


**Figure 1.** Location of the study area in the municipality of Sete Lagoas, Minas Gerais State, Brazil.

**Table 1.** Historical of soil use and management in the experimental area of Cerrado

Dates	Soil mangement		
	Disc plowing (DP)	No-tillage (NT)	Disc harrow+subsoiler (DHS)
<1995	Pasture	Pasture	Pasture
1995-2005	Corn and soybean annual succession	Corn and soybean annual succession	Corn and soybean annual succession
2006-2016	Corn cultivation	Corn and soybean rotation	Corn cultivation

with pre-accelerated Polilyte polyester resin (Reforplás T208) according to Filizola and Gomes (2004) and subjected to the making of thin and polished sections with 1.8 × 30 × 40 mm size. The micromorphological description was carried out using a Zeiss Trinocular optical microscope, Axiophot model, with an integrated digital camera, with terminologies proposed by Stoops (2003) and Stoops et al. (2018).

The porosity study was performed by micromorphometric analysis in thin sections and microtomography in undisturbed samples. In thin sections were quantified: i) percentage occupied by voids; ii) average, maximum and minimum size, and distribution of the voids from their largest axis and perimeter; iii) degree of roundness and, iv) orientation (0-180°) patterns. We used the free software Jmicrovision© 1.2.7 to measure and quantify all these attributes. The classification of pore orientation considered three classes between 0°-180° angles: 0°-29°/151°-180° (horizontal); 30°-74°/106°-150° (oblique); and 75°-105° (vertical). For the roundness void degree (RD), the Cox (1927) index was used, with a variation from 0 to 1, considering that an index closer to 1 represents more rounded. The RD adapted classification by Wadell (1933) was used considering angular (0.01 to 0.25), subangular (0.26 to 0.49), sub-rounded (0.50 to 0.70), and rounded pores (0.70 to 1). The extraction of objects to quantify the percentage of voids in the analyzed section was performed in binary images with the Magic Wand tool from the Jmicrovision© software.

For microtomography analysis, undisturbed soil samples with 75 mm diameter and 70 mm height were collected at the layer of 0.00-0.10 m using appropriate plastic boxes. The samples were kept in a humid chamber to prevent drying. The computer tomography (CT) analysis was performed in a sculpted block in the centre of the sample collected in the field, with 15 mm diameter and 25 mm high. A SKYSCAN 1174 microtomography (Bruker, Belgium) model was used for analysis, coupled with an SHT MR285MC camera. The reading conditions were 50 kV of voltage and 800 mA of electric current with an aluminum filter. The distance between camera and sample was adjusted to generate images of 32,008 pixels, with a complete rotation of 359.65° in steps of 1.4 degrees. We use the software NRecon (version 1.7.0.4) and CTAn (version 1.16.8.0) for image reconstruction and other processing.

The binarization of tomographic images consisted of defining two domains in the sample: solid particles and voids. In the porosity evaluation, just the central portion of the sample was considered, with 13.5 mm diameter and 7 mm height. The binarization considered the lower and upper limits of 35 and 255 % (grayscale threshold), respectively. We divided the porosity into open (OP) and closed porosity (CP), the latter consisting of pores that do not have connectivity. In processing the images, we calculated the Euler number, considered an indicator of connectivity (Tseng et al., 2018).

For characterization of the control soil, Oxisol under NC, macromorphological (color, structures, consistency), physical (texture, soil bulk density, porosity), chemical (pH, exchange complex, organic matter content) and mineralogical (X-Ray Diffraction) properties were analyzed (Santos et al., 2015; Teixeira et al., 2017).

Porosity (total, macro, and micro) and density (of soil and particles) analyses were performed in the NT, DHS and DP managements types to compare with the micromorphometric

results. The soil total porosity (TP) was determined from soil bulk density (Bd) and particle density (Pd) using the equation  $TP = [1 - (Bd/Pd)]$ . Soil microporosity (Mi) was determined with undisturbed samples in equilibrium to  $-0.006$  MPa in a tension table. The Macroporosity (Ma) was calculated by the difference of TP and Mi.

The granulometric analysis to determine the sand, silt, and clay fractions, and the analysis of soil bulk and particle density, macroporosity, microporosity, and total soil porosity followed the Teixeira et al. (2017) guidelines.

The soil pH was determined in  $H_2O$  in the ratio 1:2.5; H+Al by the extractor Calcium Acetate  $0.5 \text{ mol L}^{-1}$  at pH 7.0;  $Ca^{2+}$ ,  $Mg^{2+}$  and  $Al^{3+}$  extracted with  $KCl \text{ 1 mol L}^{-1}$  and Na, K and P by the Melich-1 extractor (Teixeira et al., 2017). Total organic carbon (TOC) was quantified by Walkley-Black method. Effective cation exchange capacity (CEC<sub>eff</sub>) was calculated as the sum of the bases ( $Ca^{2+}$ ,  $Mg^{2+}$ ,  $Na^+$ ,  $K^+$ , and  $Al^{3+}$ ), and total cation exchange capacity (CEC<sub>pot</sub>) was estimated by the sum of the CEC<sub>eff</sub> and potential acidity (H+Al).

The mineralogical analysis of clay fraction was carried out by X-Ray Diffraction (XDR) in Panalytical Diffractometer, Empyrean model, with CoK radiation, 45 kV and 40 mA. The scanning range was 2 to  $70^\circ 2\theta$ . We used the CrystalDiffract® demo version 6.7.3 for diffractogram interpretation.

### Statistical analyses

The data of the soil physical properties obtained were submitted to the analysis of variance (ANOVA) to verify differences among treatments after prior evaluation of normality by the Kolmogorov-Smirnov (KS) and Shapiro-Wilk tests. The Dunnett posthoc test ( $p < 0.10$ ) was then performed to compare the means of the cultivated treatments with the reference area (NC). Subsequently, the Tukey test ( $p < 0.10$ ) was used to compare the means of the cultivated treatments (NT, DHS, and DP). All statistical analysis was conducted using R software (R Development Core Team, 2017) with the support of the packages "agricolae" version 1.2-8 (Mendiburu, 2017) and "ExpDes.pt" (Ferreira et al., 2009).

## RESULTS

### Oxisol under NC: the control soil

Macroscopically, the Oxisol under NC has a strong small granular structure on Bw horizon and strong small granular to crumb structures on A horizon. These horizons have a firm (dry), friable or very friable (wet), and very plastic and sticky consistency. The A horizon presents a 5YR 4/4 (reddish-brown) dry colour and 5YR 3/3 (dark reddish-brown) wet colour, and Bw horizon has 5YR 4/4 (reddish-brown) dry colour and 5YR 3/4 (dark reddish-brown) wet colour. The transition between horizons is diffuse and wavy.

This soil has a high clay content (close to 80 %), with very clay textural class (Table 2). Due to light organic matter in topsoil, the soil bulk and particle densities are higher in Bw than A horizon. The porosity (total, macro, and micro) is high and similar in both horizons (Table 2), reiterating the Oxisol' right drainage conditions and water retention.

Chemically, this soil is acidic, dystrophic, with low contents of bases and P, moderate content of organic matter, and low clay activity (Table 2). Aluminium saturation is high, more than 50 % in the Bw horizon. The soil mineralogy highlights kaolinite, goethite, hematite, and gibbsite in the clay fraction (Figure 2). We also identified the hydroxy-Al inter-layered vermiculite (HIV). These results reiterate the high degree of soil evolution due to the latosolization process.

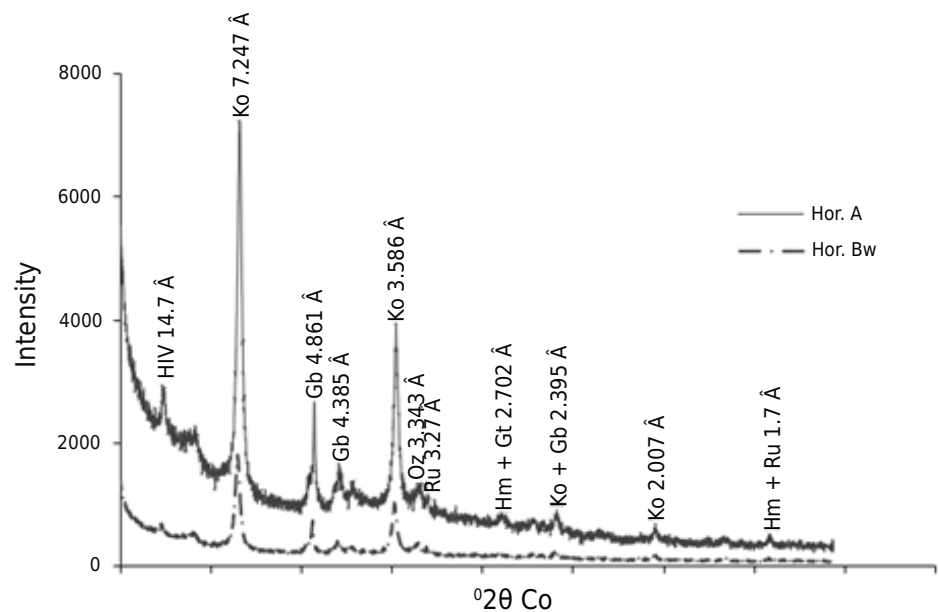
Table 3 shows the synthesis of micromorphological characterization of the *Latosolo Vermelho Distrófico* (Oxisol) under NC, NT, DHS, and DP. Figure 3 presents representative photomicrographs. The Bw horizon (0.50 m depth) has a well-developed granular

**Table 2.** Physical and chemical properties of the typical *Latosolo Vermelho Distrófico* (Oxisol) under native Cerrado (NC) vegetation

Property	Hor. A	Hor. Bw	Property	Hor. A	Hor. Bw
Bd (kg dm <sup>-3</sup> )	0.98	1.03	Ca <sup>2+</sup> (cmol <sub>c</sub> dm <sup>-3</sup> )	1.93	0.30
Pd (kg dm <sup>-3</sup> )	2.34	2.45	Mg <sup>2+</sup> (cmol <sub>c</sub> dm <sup>-3</sup> )	0.16	0.04
Microporosity (m <sup>3</sup> m <sup>-3</sup> )	0.43	0.44	Al <sup>3+</sup> (cmol <sub>c</sub> dm <sup>-3</sup> )	0.94	1.50
Macroporosity (m <sup>3</sup> m <sup>-3</sup> )	0.15	0.16	H+Al (cmol <sub>c</sub> dm <sup>-3</sup> )	8.80	7.90
Total porosity (m <sup>3</sup> m <sup>-3</sup> )	0.58	0.60	SB (cmol <sub>c</sub> dm <sup>-3</sup> )	2.13	0.36
Clay (g kg <sup>-1</sup> )	810	788	t (cmol <sub>c</sub> dm <sup>-3</sup> )	3.07	1.86
Silt (g kg <sup>-1</sup> )	50	75	T (cmol <sub>c</sub> dm <sup>-3</sup> )	10.93	8.26
Sand (g kg <sup>-1</sup> )	140	137	V (%)	19.5	4.4
pH (H <sub>2</sub> O)	4.90	4.84	m (%)	30.6	80.6
P (mg dm <sup>-3</sup> )	0.8	0.2	OM (dag kg <sup>-1</sup> )	4.94	3.93
K (mg dm <sup>-3</sup> )	16.0	11.0	P-Rem (mg L <sup>-1</sup> )	15.3	9.9

Bd: Bulk density; Pd: particle density; pH in water-ratio 1:2.5; P and K: Mehlich-1 Extractor; H+Al: calcium acetate 0.5 mol L<sup>-1</sup> - pH 7.0; t: effective cation exchange capacity; V: bases saturation index; P-Rem: remaining Phosphorus; Ca<sup>2+</sup>, Mg<sup>2+</sup>, Al<sup>3+</sup>: extractor KCl - 1 mol L<sup>-1</sup>; SB: sum of bases; T: cation exchange capacity at pH 7.0; m: aluminum saturation index; OM (organic matter) = Org. C. × 1.724 - Walkley - Black.

microstructure. The aggregates are smaller than 500 μm, well separated by a complex packing void system. The groundmass is composed of a reddish-brown micromass, with undifferentiated or granostriated b-fabric. The coarse materials are composed of fine sand-sized quartz grains and opaque minerals. The aggregates are individualized from each other, and among them, there are quartz grains of medium sand size, characterizing an enaulic relative distribution.


**Figure 2.** X-ray diffraction patterns of clay fraction of a *Latosolo Vermelho Distrófico* in Cerrado (Co $\alpha$  radiation). HIV: Hydroxy-Interlayered Vermiculite; Ko: Kaolinite; Gb: Gibbsite; Qz: Quartz; Ru: Rutile; Hm: Hematite; Gt: Goethite.

**Table 3.** Micromorphological characterization at depths 0 (surface), 0.10 and 0.50 m of a typical *Latossolo Vermelho Distrófico* under native Cerrado (NC) and types of management cultivated for more than two decades under no-tillage (NT), use of disc harrow+subsoiler (DHS) and use of disc plowing (DP)

Type of management	Depth	Microstructure	Groundmass			Organic compounds	Soil features
			Coarse Material	Micromass	c/f <sub>2µm</sub> relative distribution		
NC	Surface	Well to moderately separated granular. Moderately separated subangular blocks, formed by coalesced granules. Compound packing voids.	Subangular quartz grains, fine sand, and opaque minerals	Dark brown to reddish-brown, undifferentiated to granostriated b-fabric	Enaulic	Roots, root traces, humified organic matter, coal and nodules	Typical ferruginous nodules and loose continuous infillings
	0.10 m	Well separated granular. Moderately separated subangular blocks, formed by coalesced granules. Complex packing voids.	Subangular quartz grains, fine sand, and opaque minerals	Reddish-brown, undifferentiated to granostriated b-fabric	Enaulic	Roots, root traces, humified organic matter, coal and nodules	Typical ferruginous nodules and loose continuous infillings
	0.50 m	Rounded well separated granular. Complex packing voids.	Subangular quartz grains, fine sand, and opaque minerals	Reddish-brown to reddish-yellow, undifferentiated to granostriated b-fabric	Enaulic	Root traces, humified organic matter, coal and nodules	Typical ferruginous nodules and loose continuous infillings
NT	Surface	Vughy with little or not at all connected voids, without noticeable aggregates. Rounded to subrounded voids, with circular orientation. There are also root channels	Subrounded to rounded quartz grains, fine to medium sand, and opaque minerals	Reddish-brown with some yellowish-red portions, undifferentiated b-fabric	Porphyric	Roots, organic punctuations in micromass and charcoal	Typical ferruginous nodules
	0.10 m	Moderately separated subangular blocks, with planar voids. Also occur vughs with poorly connected voids.	Subrounded to rounded quartz grains, fine to medium sand, and opaque minerals	Brown to reddish-brown, undifferentiated b-fabric	Porphyric	Roots, traces of roots, organic punctuations in micromass and charcoal	Typical ferruginous nodules
	0.50 m	Well to moderately separated granular. Compound packing voids.	Subrounded quartz grains, fine to medium sand, and opaque minerals	Dark brown to reddish-brown, undifferentiated to granostriated b-fabric	Enaulic	Organic punctuations, coal and nodules	Typical and concentric ferruginous nodules
GHS	Surface	Moderately separated granular. Moderately separated subangular blocks. Compound packing voids and vughs.	Subrounded quartz grains, fine to medium sand, and opaque minerals	Dark brown, undifferentiated to granostriated b-fabric	Enaulic-porphyric	Traces of roots, organic punctuations in the micromass, nodules and charcoal	Typical ferruginous nodules
	0.10 m	Poorly separated subangular blocks. Vughy with poorly connected pores. The vughs are rounded to subrounded, and, in some cases, oriented.	Subrounded quartz grains, fine to medium sand, and opaque minerals	Reddish to reddish-brown, undifferentiated b-fabric	Porphyric	Traces of roots, organic punctuations in the micromass, nodules and charcoal	Typical ferruginous nodules
	0.50 m	Vughy with poorly connected pores. The vughs are rounded to subrounded, and shown circular orientation. Poorly separated subangular blocks, with planar voids.	Subrounded quartz grains, fine to medium sand, and opaque minerals	Reddish to reddish-brown, undifferentiated b-fabric	Porphyric	Organic material soaking the micromass and charcoal	Typical ferruginous nodules
DP	Surface	Poorly separated planar microstructure, with voids of major axis parallel to the surface. Subordinately, angular blocks, poorly separated, with planar voids.	Subrounded quartz grains, fine to medium sand, and opaque minerals	Reddish-brown, undifferentiated to monostriated b-fabric	Porphyric	Traces of roots, organic punctuations in the micromass, and charcoal	-
	0.10 m	Poorly separated planar microstructure, with voids of a major axis parallel to the surface. Poorly separated angular blocks, with planar voids.	Subrounded quartz grains, fine to medium sand, and opaque minerals	Reddish-brown, undifferentiated to monostriated b-fabric	Porphyric	Traces of roots, organic punctuations in the micromass, and charcoal	Typical ferruginous nodules
	0.50 m	Moderately separated granular. Complex packing voids	Subrounded quartz grains, fine to medium sand, and opaque minerals	Dark brown, undifferentiated to granostriated b-fabric	Enaulic	Organic material soaking the micromass and charcoal	Typical ferruginous nodules

The main pedofeatures are continuous loose infillings and typical ferruginous nodules. Organic matter occurs as amorphous organic fine material, organic nodules, and root fragments in different oxidation degrees. Charcoal fragments are observed inside the granular aggregates, with tiny size ( $<100\ \mu\text{m}$ ), or between aggregates, with coarse sand size.

In both depths (0.00-0.05 and 0.10-0.15 m), the A horizon has organo-mineral nature, in which the mineral constituents already described are mixed with living or decomposing organic materials (Figure 3). The well-developed granular and sub-rounded block microstructures occur. These blocks are internally composed of coalesced granules, constituting a bi-modal structure. Ferruginous and organic nodules are also present, being organic ones the most common. Continuous loose infillings occur associated with biological pedofeatures, with small round excrements and granular aggregates inside them.

### NT, DHS, and DP soil management types

Table 3 and figure 3 shows, respectively, the synthesis of micromorphological characterization and representative photomicrographs. We present the comparative descriptions for 0.00-0.05, 0.10-0.15 and 0.50-0.55 m layers in the three soil management types studied.

In no-tillage management, the surface has microstructures characterized by the predominant void systems, mainly poorly connected cavities with rounded to sub-rounded shapes. In some portions of the thin sections, it is possible to recognize moderately separated small rounded blocks with planar voids. At 0.50 m depth, the microstructure is quite distinct from the surface, with small, rounded, moderately separated granular aggregates, similar to NC control soil. The relative distribution of the groundmass is porphyric on the surface and enaulic in depth. The groundmass is composed of quartz and opaque minerals as coarse material and of brown-reddish to dark-brownish micromass with undifferentiated b-fabric.

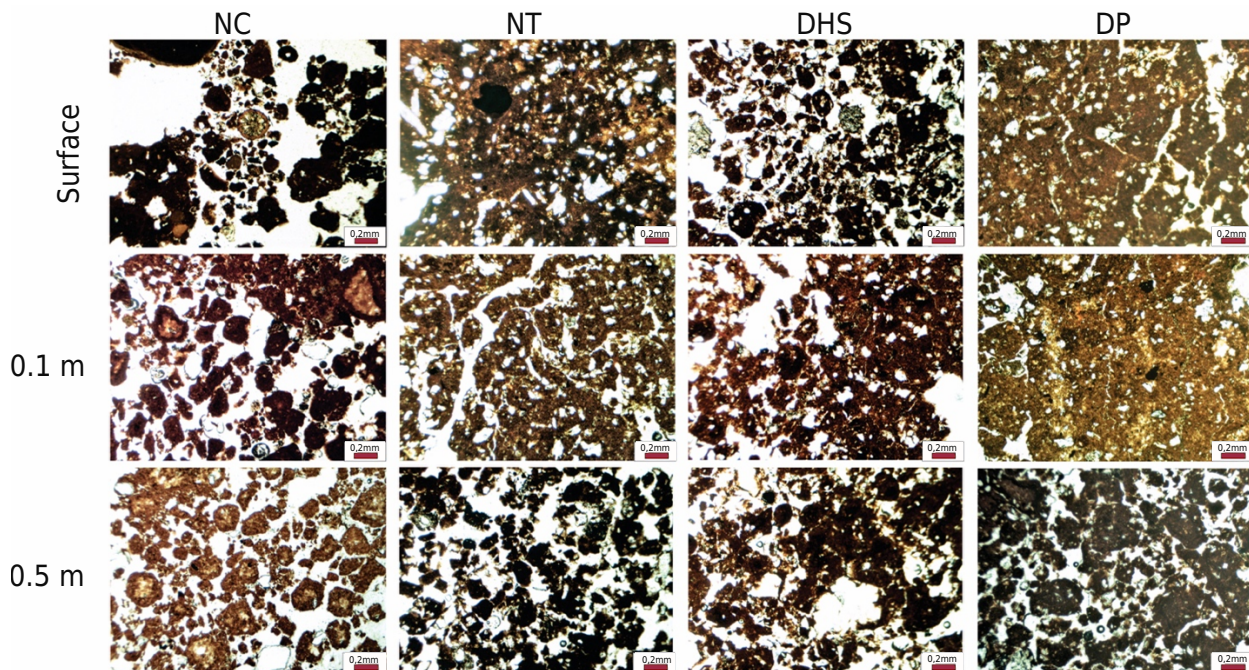


**Figure 3.** Photomicrographs obtained in a petrographic microscope with polarizing light, parallel nicols representative of the microstructures present at depths 0 (surface), 0.10 and 0.50 m of the typical *Latosolo Vermelho Distrófico* (Oxisol) under native Cerrado (NC) and the types of management cultivated for more than two decades with no-tillage (NT), use of Disc Harrow+Subsoiler (DHS) and use of disc plowing (DP). 4X lens.

In the disc harrow+subsoiler management, the granular microstructure is predominant at 0.00-0.05 m soil layer. The aggregates are separated from each other by a compound packing void system. At the subsequent layers, 0.10-0.15 and 0.50-0.55 m, two distinct microstructures occur, respectively, subangular blocks and cavities, in which the aggregates are not easily separated, and the voids are more closed, with little or no connection. Some planar voids can be identified at 0.50 m depth. The groundmass composition fund remains the same in all horizons, with a change in the c/f ratio and relative distributions (Table 3), porphyrenaulic at 0.10-0.15 m layer, and only porphyric below that.

In disc plowing management, at 0.10 m depth, occurs subangular blocks and, mainly, fissure microstructure, containing planar voids poorly connected with the largest axis oriented parallel to the surface. The relative distribution is porphyric, in which quartz grains and charcoal fragments with fine to medium sand size occur immersed in the reddish micromass. At 0.50 m depth, the microstructure is similar to NC control soil, with small rounded granular aggregates and an enaulic relative distribution. The most common pedofeatures is orthic ferruginous nodules, with internal fabric similar to the around groundmass.

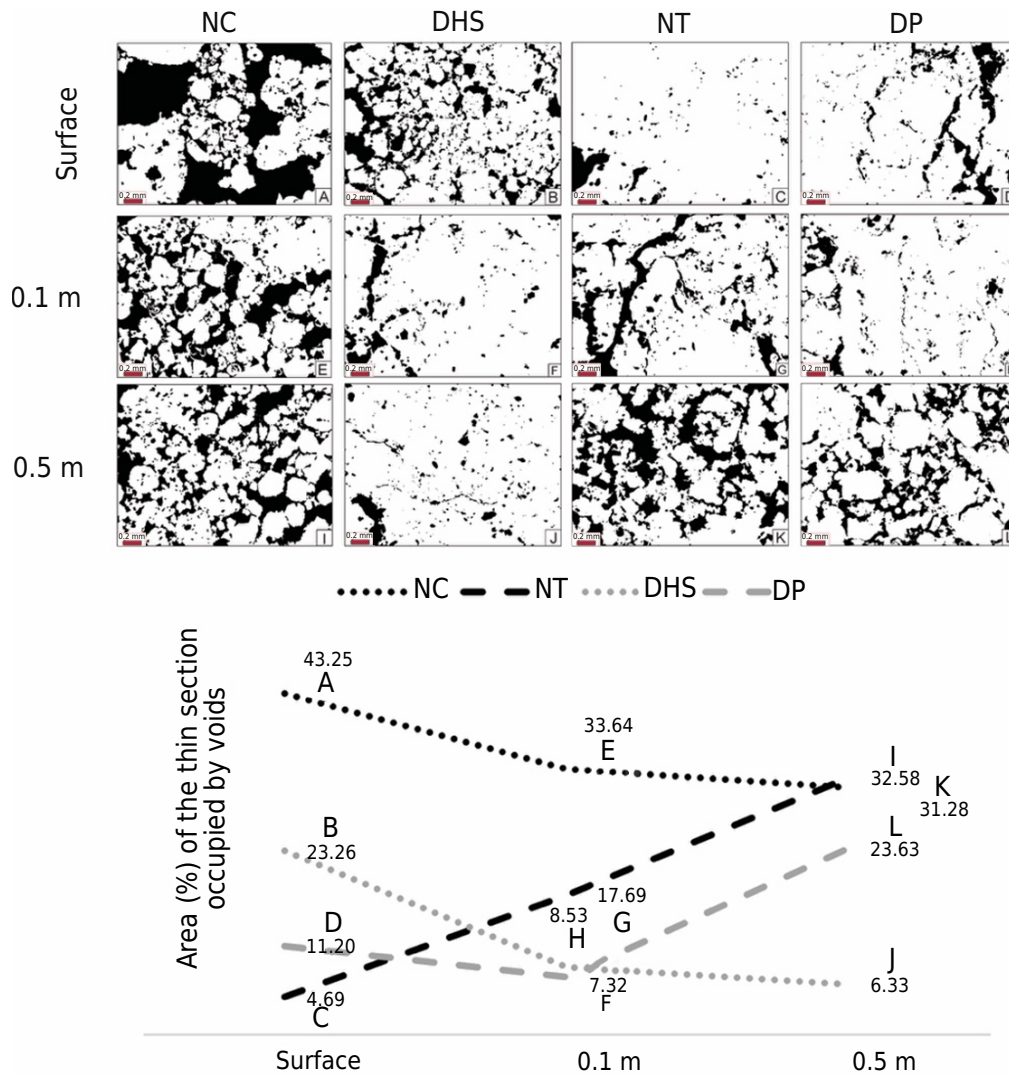


**Figure 4.** Characterization of porous system on the surface (upper, SUP), 0.10 and 0.50 m of depth in evaluated soil (NC: Native Cerrado, DHS: Disc Harrow+Subsoiler, NT: No-Tillage, DP: disc plowing).

## Porosity characterization

The results of micromorphometric characterization of the porous system in the different treatments are shown in figures 3, 4, and 5. Similarly, table 4 presents the results of the soil porosity characterization by classic laboratory methods, aiming at comparison with those obtained by CT.

Considering the percentage of area occupied by voids in the thin sections (Figure 4), NC control soil and DHS soil management show a reduction with depth. We observe an opposite behavior in NT and DP management, with the porosity increasing in depth. The NC has a greater porosity than all three soil management types. These results are corroborated by total porosity obtained in the laboratory (Table 4), where the values for 0.10-0.15 and 0.50-0.55 m layers are lower in management types than in the control soil.

The void size (Figure 5a) increases in depth in the NC, NT, and DP managements. Only DHS showed a reduction. In the length of the longest axis, this reduction was from 0.04 mm on the surface to 0.026 mm at 0.50 m depth. The reduction was from 1.14 to 0.07 mm according to the perimeter values. We observed larger voids on the surface of NC control soil and DHS management. In the NT and DP, they occur in greater depth. No direct relationship was observed between the predominance of planar pores and larger pores, demonstrating that packing systems voids can also contribute to these results.

Considering the 0.05 mm limit for separation of the micro and meso/macropores, the NC control soil shows a more diversified distribution along with the profile, in which macro and micropores are present in all depths. In soil management types, the presence of micropores is more significant in NT and DP, especially at 0.00-0.05 and 0.10-0.15 m soil layers and at 0.50 m depth in DHS. Macropores are common in DHS surface and at the highest depth of NT and DP.

Thus, in both analyses, micromorphometric (Table 3) and laboratory (Table 4), the increased micropores on the surface are associated with the reduction of soil's macroporosity. No macroporosity is verified at 0.10 m depth in all soil management types. However, macroporosity is slightly more preserved in 0.50 m depth, not differing from the control soil. In laboratory results, only DHS management does not show macroporosity reduction

**Table 4.** Physical characteristics analyzed by laboratory methods at 0.10 and 0.50 m of depths at a typical *Latossolo Vermelho Distrófico* (Oxisol) under native Cerrado (NC) and managements cultivated for more than two decades with No-Tillage (NT), use of Disc Harrow+Subsoler (DHS) and Disc Plowing (DP)

Treatments	kg dm <sup>-3</sup>		m m <sup>-3</sup>		
	Bd	Pd	Mi	Ma	TP
0.10 m					
NC	0.98	2.34	0.43	0.15	0.58
NT	1.37 *ab	2.54	0.46 *	0.01 *	0.47 *
DHS	1.28 *b	2.43	0.47 *	0.00 *	0.47 *
DP	1.30 *a	2.50	0.48 *	0.01 *	0.49 *
CV (%)	2.80	4.10	2.40	44.80	3.90
0.50 m					
NC	1.03	2.45	0.44	0.16	0.60
NT	1.26 *a	2.58	0.44	0.07	0.51 *
DHS	1.15 b	2.55	0.42	0.13	0.55
DP	1.03	2.45	0.44	0.16	0.60
CV (%)	4.50	2.80	4.00	37.40	4.70

Bd: Bulk density; Pd: Particle density; Mi: soil microporosity; Ma: soil macroporosity; TP: soil total porosity; CV: Coefficient of Variation; (\*) different from NC by Dunnett's test ( $p < 0.1$ ); different letters on the line differ from each other by the Tukey test ( $p < 0.1$ ).

at 0.50 m depth. These differences between micromorphometric and laboratory analysis can indicate a spatial variability in the compaction in the depth of the DHS management. The porosity results obtained in the laboratory or thin sections were generally consistent, despite the undisturbed samples collected in a single position. In contrast, a more significant number of samples was used to express an average value for the laboratory analysis.

The roundness void degree (Figure 5b) shows a more excellent distribution of pore types (subangular, sub-rounded, and rounded) in the NC control soil and the predominance of rounded voids in management types. When compared to the size from the length on the longest axis (Figure 5c), considering voids up to 1 mm in length, we observed that the smaller the pore, the more rounded they are. This behavior suggests the impact of compaction on the macropore's shape.

The pore orientation (Figure 6) showed a similar distribution in all depths on NC and management types. The pore classification indicated a predominance of vertical and oblique pores, especially in the layers with packing void systems. Comparatively, the NT and DP managements showed a slight increase in the percentage of horizontal pores in the upper layers, whereas in DHS this increase was greater than 0.10 m depth.

The tomographic images (Figure 7) show the greatest porosity (colored part of the images) in the NC soil control, followed by DHS management. In quantitative terms, we obtained  $0.69 \text{ m}^3 \text{ m}^{-3}$  for NC,  $0.07 \text{ m}^3 \text{ m}^{-3}$  for DP,  $0.04 \text{ m}^3 \text{ m}^{-3}$  for NT and  $0.28 \text{ m}^3 \text{ m}^{-3}$  for DHS. These values are not consistent with the laboratory results for management types (Table 4) and more approximated for NC control soil. Because of the problems with the cultivation areas, the analysis of open (OP) and closed (CP) porosity was impaired. In this sense, only the values obtained for the NC seem more reliable, in which the technique revealed that 99.93 % of the voids were open; that is, they present connectivity with the others.

According to their diameter (Figure 8), the void distribution indicates a void curve with displacement to the left in the management types. This distribution indicates gains in microporosity, corroborating with the other analysis. However, the significant reduction of pores in NT and DP management, possibly due to the problems already mentioned, makes greater considerations difficult.

The Euler number associated with the control soil and managements were: -4523 (NC), 6371 (DP), 7023 (NT), and -6519 (DHS). Negative values are associated with more excellent void connectivity, while positive values indicate void discontinuity. Thus, CN and DHS showed better soil quality in terms of voids space. Again, problems with the technique can limit the use of these results.

## DISCUSSION

### Oxisol under NC: the control soil

Granular aggregates in *Latossolos* derived from limestone under Native Cerrado have already been described by other authors (Ferreira et al., 1999; Schaefer, 2001). They represent very weathered soils, with kaolinitic-gibbsitic composition and red color, even if the iron content is low. This mineral assemblage and the long-term biological activity, mainly by termites, are responsible for the granular aggregate's formation. According to Schaefer (2001), the combined action of physicochemical conditions created by clay mineralogy and the production and stabilization of texturally selected particles by bioturbation promote the microstructural organization of uniformly arranged constituents in small, stable, rounded micro-granular aggregates.

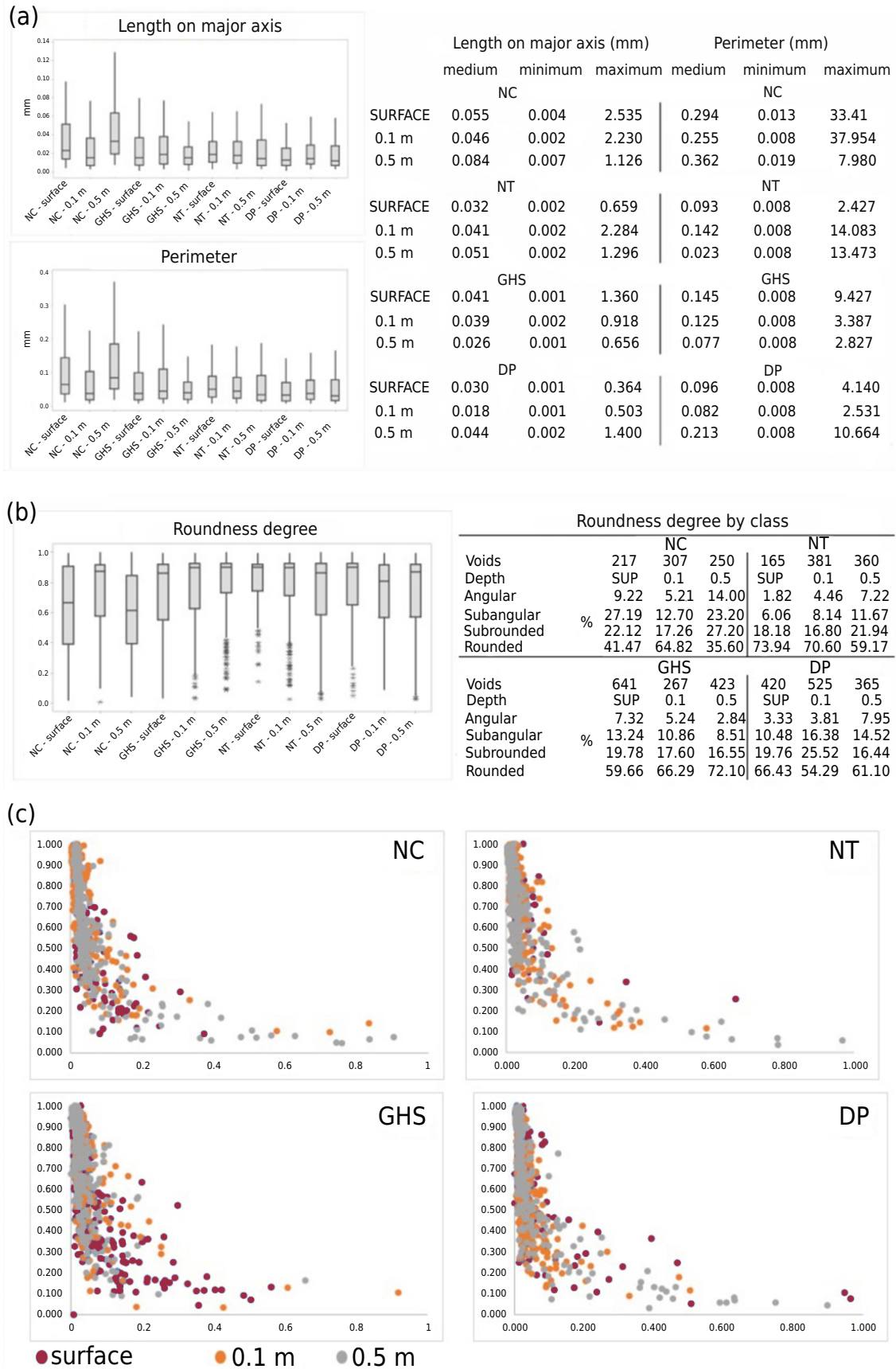


**Figure 5.** Morphometric characteristics of soil pores: length of the longest axis and perimeter of pores (a); porous classes as to the degree of roundness (b) and relationship between the degree of roundness and the length of the pores in its longest axis (c) in the evaluated uses and management of the soil (NC: Native Cerrado; DHS: Subsoiling Grid; NT: No-Tillage; DP: disc plowing).

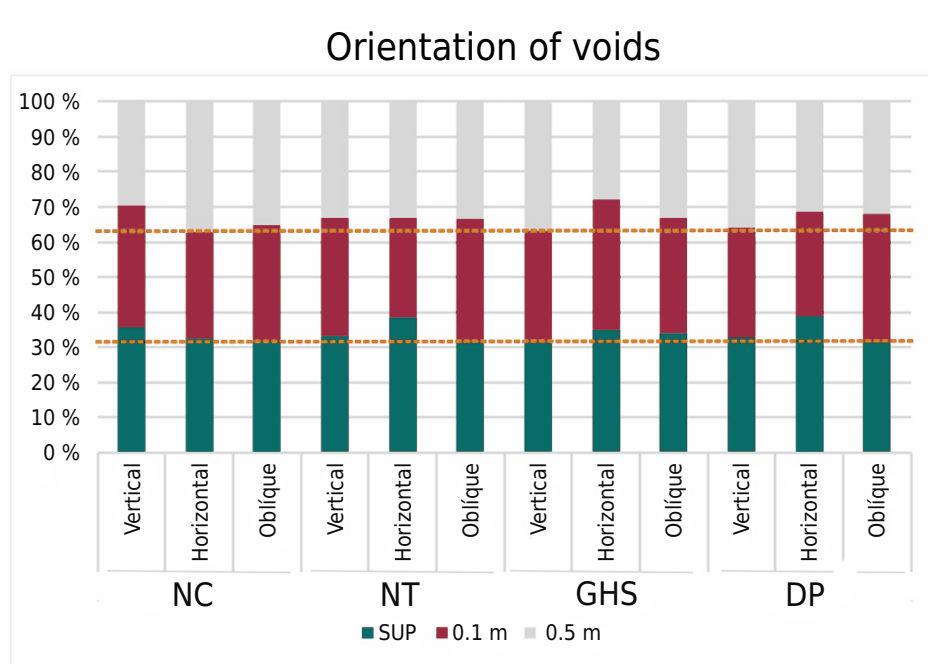


**Figure 6.** Percentage of pore orientation classes in the control soil (NC) and management types (NC: Native Cerrado; DHS: Subsoiling Grid; NT: No-Tillage; DP: disc plowing). The dashed red lines indicate the transition between classes.

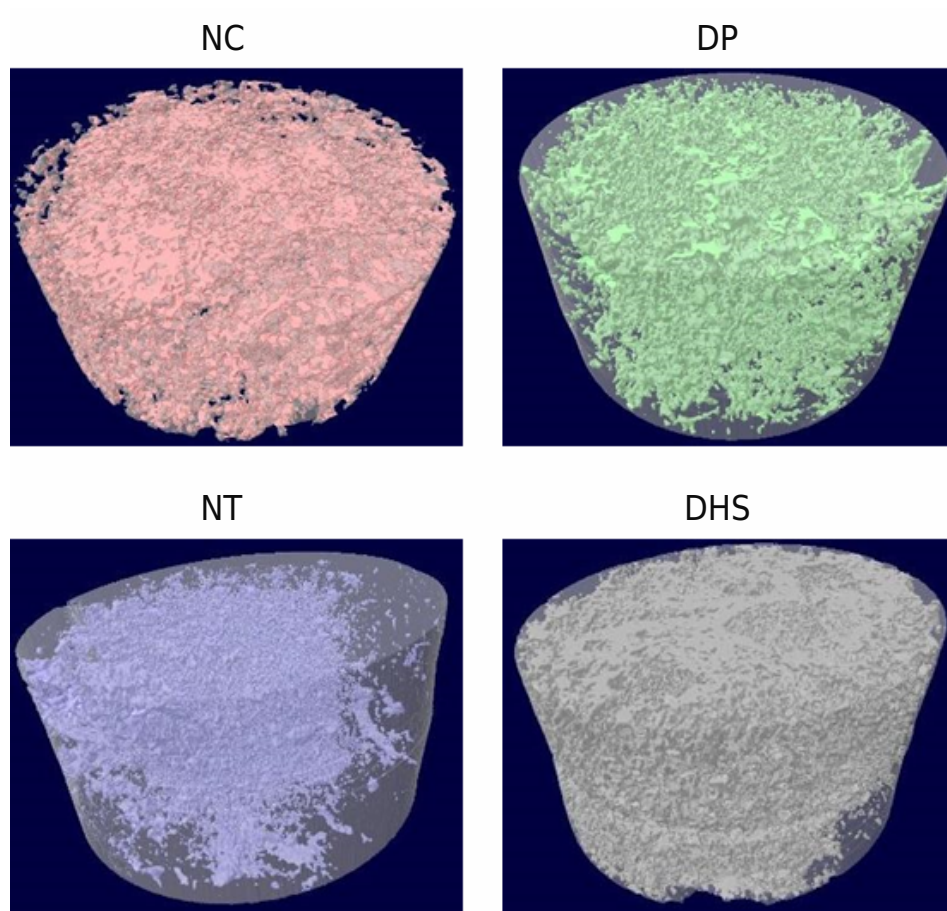


**Figure 7.** Representation of the pore network in the specimens representative of the uses and management of native Cerrado soil (NC), disc plowing (DP), no-tillage (NT) and disc harrow+subsoiler (DHS).

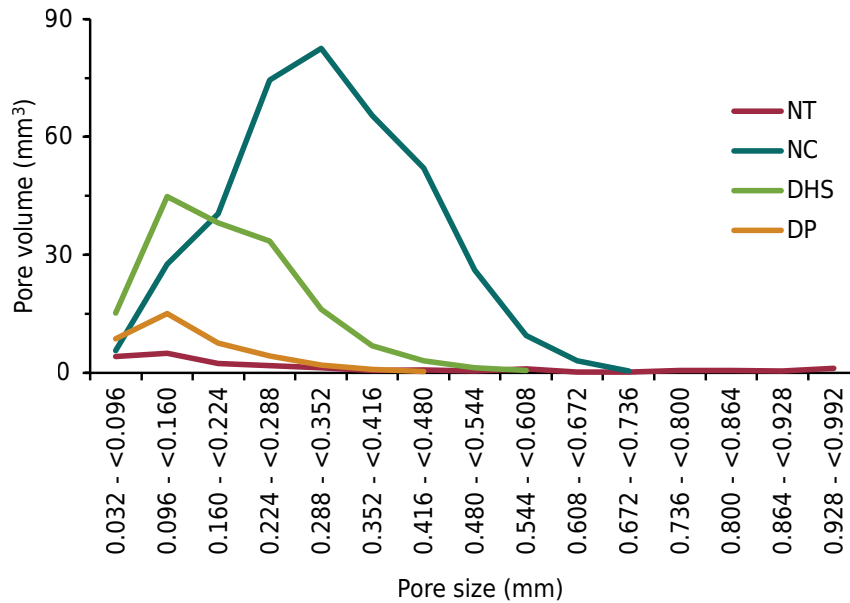


**Figure 8.** Pore size distribution according to its diameter in different uses and soil management evaluated based on the computed tomography technique in the 0.00-0.10 m layer. NC: Native Cerrado; DHS: Subsoiling Grid; NT: No-Tillage; DP: disc plowing.

### NT, DHS, and DP soil management types

The changes in soil are analyzed based on the specificities of each management type. The NT and DP showed more soil compaction on the surface layer, whereas this compaction occurred in-depth at the DHS management (Figure 4). The no-tillage system is considered the best agricultural technology adopted in Brazil during the last 50 years (Giarola et al., 2013). However, it can cause structural changes when not applied correctly, such as the soil compaction observed in this study. Nonetheless, some studies have found that reduced cultivation alone was not able to improve soil structure (Luz et al., 2022). The superficial compaction in this cultivation system has been considered an increasing problem in agriculture, intensified by the frequent use of agricultural machinery (Reichert et al., 2009; Nunes et al., 2015). In Paraná, a Brazilian state with a sizeable no-tillage adoption, machine traffic under high soil moisture conditions is considered the main responsible for soil compaction (Tavares Filho and Tessier, 2010). On the other hand, when adopted correctly, this system promotes changes in the soil structure associated with a vast network of cracks that lead to more soil moisture retention, stimulating biological activity, as well as a greater abundance of roots (Tavares Filho et al., 2001), which favors the soil physical quality.

At a depth of 0.10 m of DHS and DP treatments, the thin blades indicated reduced porosity, which is not very consistent with the turning provided by these implements at that depth. Compaction of plows and harrows is most often reported below the depth of preparation, as in the study of Bertolino et al. (2010), who observed in a conventional soil management system in Rio de Janeiro State that the use of disc plows followed by harrowing provided the formation of a compacted layer close to 0.20 m in depth associated with a 44 % reduction in total porosity from the soil. Although stable, the granular aggregates can be modified by soil management adopted, mainly later than two decades, as observed in this study. Compaction is the primary mechanism of structure deformation, which implies a decrease in macropores and, consequently, reduces the water infiltration rates and oxygen diffusion to the roots, in addition to the increased mechanical impediment. As Kilasara and Tessier (1991) observed, soil porosity was the better indicator for evaluating the structure's degradation.

### Porosity characterization

There are several studies in the literature that evaluate the impacts of soil management on porosity. Some of these studies point to greater water availability, pore network and connectivity in reduced tillage systems (Eden et al., 2020). Similar to what was found in the present study, macroporosity in NT showed a decrease in the surface layer of soil compared to management with conventional cropping system (Wardak et al., 2022). We found a reduction of total porosity in managements compared to the control soil at 0.10 m depth (Table 3). At 0.50 m depth, only NT management presented porosity reduction. The loss of total porosity reflects the breakdown of aggregates and the macro into micropores transformation (Soares et al., 2005).

### Micromorphological techniques

Micromorphology techniques improved the understanding of changes in soil structure under different soil management. Our study demonstrated the compatibility of laboratory and micromorphology results, similar to that verified by Cooper (1999) and Souza et al. (2006). However, computed tomography presented limitations to soil structure assessment, which were associated with the higher soil bulk density of the cultivated areas. A possible explanation for these limitations is the effect of soil compaction on the attenuation coefficient (Pedrotti et al., 2003). Compacted soil limits the X-rays transmission, impairing the resolution and accurate estimation of the soil porosity.

We observed the granular aggregates' destruction and soil compaction regardless of the type of management adopted. Micromorphological indicators of these findings are: i) modifications in relative distribution, from enaulic to porphyric; ii) modification in the void systems, from packaging to cavitary and/or planar, and iii) modifications in the microstructures, from granular to subangular blocks or apedic microstructures, defined by the predominant void system, such as cavitary or fissural. These modifications in micromorphological scale reinforce the possibility of changes in the physical, hydrological, and biological conditions of *Latossolos* (Oxisols) (Juhász et al., 2007).

## CONCLUSIONS

Long-term cultivation under disc harrow+subsoiler provides less reduction of soil total porosity than under no-tillage (NT) and disc plowing (DP) in the superficial layer of the Cerrado Oxisol (*Latossolo*). Micromorphology technique allows identifying microstructural changes caused by the management of Oxisols (*Latossolos*) of small and strong granular structures. Even so, the relative good resistance of the aggregates of the soils with granular structure is evident even after two decades of handling, which corroborates the morphological classification regarding the degree of development of these structures.

## ACKNOWLEDGEMENTS

The authors are grateful for the financial support of the Fundação de Amparo à Pesquisa do Estado de Minas Gerais-FAPEMIG-Brasil (Code APQ-00887-17) and Coordenação de Aperfeiçoamento de Pessoal de Nível Superior (CAPES, Brasil, Finance Code 001). We thank also to the PEC-PG (Programa Estudantes Convênio de Pós-Graduação) for the scholarship to the first author; to the Conselho Nacional de Desenvolvimento Científico e Tecnológico (CNPq) for the support; the Brazilian Agricultural Research Corporation (Embrapa) for partnership and support in the experimental area, and to "Núcleo de Microscopia e Microanálise" (NMM, UFV) for the CT facilities provided by FINEP/FAPEMIG and CNPq.

## REFERENCES

- Bertolino AVFA, Fernandes NF, Miranda JPL, Souza AP, Lopes MRS, Palmieri F. Effects of plough pan development on surface hydrology and on soil physical properties in Southeastern Brazilian plateau. *J Hydrol.* 2010;393:94-104. <https://doi.org/10.1016/j.jhydrol.2010.07.038>
- Brandalise LA, Pimentel GB, Steiner HP, Soares J, Mendes JR, Queiroz NF, Lima OM, Pádua W. Projeto sondagens Bambuí em Minas Gerais: Relatório final. Belo Horizonte: DNPM/CPRM; 1980.
- Cooper M. Influência das condições físico-hídricas nas transformações estruturais entre horizonte B latossólico e B textural sobre diabásio [thesis]. Piracicaba: Universidade de São Paulo; 1999.
- Costa MT, Branco JJR. Roteiro para a excursão Belo Horizonte - Brasília. In: Branco JJR, editor. Contribuição ao 14° Congresso Brasileiro de Geologia. Belo Horizonte, Instituto de Pesquisas Radioativas; 1961. p. 9-25. (Publicação n. 15).
- Cox EP. A method for assigning numerical and percentage values to the degree of roundness of sand grains. *J Paleontol.* 1927;1:179-83.
- Eden M, Bachmann J, Cavalari C, Kostopoulou S, Kozaiti M, Böttcher J. Soil structure of a clay loam as affected by long-term tillage and residue management. *Soil Till Res.* 2020;204:104734. <https://doi.org/10.1016/j.still.2020.104734>
- Ferreira EB, Cavalcanti P, Nogueira DA. Função em código R para analisar experimentos em DBC simples, em uma só rodada. In: Resumos da II Jornada Científica da Universidade Federal de Alfenas-MG, 2009, Alfenas. Alfenas: Unifal-MG; 2009.
- Ferreira MM, Fernandes B, Curi N. Influência da mineralogia da fração argila nas propriedades físicas de latossolos da região sudeste do Brasil. *Rev Bras Cienc Solo.* 1999;23:515-24. <https://doi.org/10.1590/s0100-06831999000300004>
- Ferreira TR, Pires LF, Wildenschild D, Heck RJ, Antonino ACD. X-ray microtomography analysis of lime application effects on soil porous system. *Geoderma.* 2018;324:119-30. <https://doi.org/10.1016/j.geoderma.2018.03.015>
- Fichtner T, Goersmeyer N, Stefan C. Influence of soil pore system properties on the degradation rates of organic substances during soil aquifer treatment (SAT). *Appl Sci.* 2019;9:496. <https://doi.org/10.3390/app9030496>
- Filizola HF, Gomes MAF. Coleta e impregnação de amostras de solo para análise micromorfológica. Jaguariúna: Embrapa Meio Ambiente; 2004.
- Gerzabek MH, Stoops G, Ottner F, Wang SL, Huang LS, Zehetner F. The evolution of soil microstructure and micromineralogy along a soil age gradient on the Galápagos Islands (Ecuador). *Geoderma Reg.* 2023;32:e00609. <https://doi.org/10.1016/j.geodrs.2023.e00609>
- Giarola NFB, Silva AP, Tormena CA, Guimarães RML, Ball BC. On the visual evaluation of soil structure: The Brazilian experience in Oxisols under no-tillage. *Soil Till Res.* 2013;127:60-4. <https://doi.org/10.1016/j.still.2012.03.004>
- Juhász CEP, Cooper M, Cursi PR, Ketzner AO, Toma RS. Savanna woodland soil micromorphology related to water retention. *Sci Agric.* 2007;64:344-54. <https://doi.org/10.1590/S0103-90162007000400005>
- Kilasara M, Tessier D. Intérêt des mesures physiques sur échantillons non remaniés dans la caractérisation des sols ferrallitiques. Application à la couverture ferrallitique du district de Muhesa (Tanzanie). Paris: Cahier ORSTOM Série Pédologie. 1991;26:91-103.
- Lawrence M, Jiang Y. Porosity, pore size distribution, micro-structure. In: Amziane S, Collet F, editors. Bio- aggregates based building materials. Dordrecht: Springer; 2017. p. 39-71. [https://doi.org/10.1007/978-94-024-1031-0\\_2](https://doi.org/10.1007/978-94-024-1031-0_2)
- Luz FB, Carvalho ML, Castioni GAF, Bordonal RO, Cooper M, Carvalho JLN, Cherubin MR. Soil structure changes induced by tillage and reduction of machinery traffic on sugarcane - A diversity of assessment scales. *Soil Till Res.* 2022;223:105469. <https://doi.org/10.1016/j.still.2022.105469>

- Malobane ME, Nciizah AD, Bam LC, Mudau FN, Wakindiki IIC. Soil microstructure as affected by tillage, rotation and residue management in a sweet sorghum-based cropping system in soils with low organic carbon content in South Africa. *Soil Till Res.* 2021;209:104972. <https://doi.org/10.1016/j.still.2021.104972>
- Mendiburu F. *Agricolae: Statistical procedures for agricultural research.* (Version 1.2-8) [internet]. 2017. Available from: <https://cran.r-project.org/web/packages/agricolae/index.html>
- Meurer K, Barron J, Chenu C, Coucheney E, Fielding M, Hallett P, Herrmann AM, Keller T, Koestel J, Larsbo M, Lewan E, Or D, Parsons D, Parvin N, Taylor A, Vereecken H, Jarvis N. A framework for modelling soil structure dynamics induced by biological activity. *Glob Change Biol.* 2020;26:5382-403. <https://doi.org/10.1111/gcb.15289>
- Nunes MR, Denardin JE, Pauletto EA, Faganello A, Pinto LFS. Effect of soil chiseling on soil structure and root growth for a clayey soil under no-tillage. *Geoderma.* 2015;259-260:149-55. <https://doi.org/10.1016/j.geoderma.2015.06.003>
- Or D, Keller T, Schlesinger WH. Natural and managed soil structure: On the fragile scaffolding for soil functioning. *Soil Till Res.* 2021;208:104912. <https://doi.org/10.1016/j.still.2020.104912>
- Pedrotti A, Pauletto EA, Crestana S, Cruvinel PE, Vaz CMP, Naime JM, Silva AM. Tomografia computadorizada aplicada a estudos de um Planossolo. *Pesq Agropec Bras.* 2003;38:819-26. <https://doi.org/10.1590/S0100-204X2003000700005>
- R Development Core Team. *R: A language and environment for statistical computing.* Vienna, Austria: R Foundation for Statistical Computing; 2017. Available from: <http://www.R-project.org/>
- Reichert JM, Kaiser DR, Reinert DJ, Riquelme UFB. Variação temporal de propriedades físicas do solo e crescimento radicular de feijoeiro em quatro sistemas de manejo. *Pesq Agropec Bras.* 2009;44:310-9. <https://doi.org/10.1590/S0100-204X2009000300013>
- Santos HG, Jacomine PKT, Anjos LHC, Oliveira VA, Lumbrreras JF, Coelho MR, Almeida JA, Araújo Filho JC, Oliveira JB, Cunha Tjf. *Sistema brasileiro de classificação de solos.* 5. ed. rev. ampl. Brasília, DF: Embrapa; 2018.
- Santos RD, Santos HG, Ker JC, Anjos LHC, Shimizu SH. *Manual de descrição e coleta de solo no campo.* 7. ed. rev. ampl. Viçosa, MG: Sociedade Brasileira de Ciência do Solo; 2015.
- Schaefer CER. Brazilian latosols and their B horizon microstructure as long-term biotic constructs. *Soil Res.* 2001;39:909-26. <https://doi.org/10.1071/sr00093>
- Shen J, Wang Q, Chen Y, Han Y, Zhang X, Liu Y. Evolution process of the microstructure of saline soil with different compaction degrees during freeze-thaw cycles. *Eng Geol.* 2022;304:106699. <https://doi.org/10.1016/j.enggeo.2022.106699>
- Soares JLN, Espindola CR, Foloni LL. Alteração física e morfológica em solos cultivados com citros e cana-de-açúcar, sob sistema tradicional de manejo. *Cienc Rural.* 2005;35:353-9. <https://doi.org/10.1590/s0103-84782005000200016>
- Souza ZM, Júnior JM, Cooper M, Pereira GT. Micromorfologia do solo e sua relação com atributos físicos e hídricos. *Pesq Agropec Bras.* 2006;41:487-92. <https://doi.org/10.1590/S0100-204X2006000300016>
- Stoops G. *Guidelines for analysis and description of soil and regolith thin sections.* Madison, Wisconsin: Soil Science Society of America; 2003. <https://doi.org/10.1111/j.1351-0754.2004.00591b.x>
- Stoops G, Marcelino V, Mees F. *Interpretation of micromorphological features of soils and regoliths.* 2nd ed. Amsterdam: Elsevier; 2018.
- Tang CS, Cheng Q, Gong X, Shi B, Inyang HI. Investigation on microstructure evolution of clayey soils: A review focusing on wetting/drying process. *J Rock Mech Geotech Eng.* 2023;15:269-84. <https://doi.org/10.1016/j.jrmge.2022.02.004>
- Tavares Filho J, Barbosa GMC, Guimarães MF, Fonseca ICB. Resistência do solo à penetração e desenvolvimento do sistema radicular do milho (*Zea mays*) sob diferentes sistemas de manejo em um Latossolo Roxo. *Rev Bras Cienc Solo.* 2001;25:725-30. <https://doi.org/10.1590/S0100-06832001000300022>

- Tavares Filho J, Tessier D. Effects of different management systems on porosity of Oxisols in Parana, Brazil. *Rev Bras Cienc Solo*. 2010;3:899-906. <https://doi.org/10.1590/S0100-06832010000300031>
- Teixeira PC, Donagemma GK, Fontana A, Teixeira WG. Manual de métodos de análise de solo. 3. ed. rev e ampl. Brasília, DF: Embrapa; 2017.
- Tseng TL, Alves MC, Crestana S. Quantifying physical and structural soil properties using X-ray microtomography. *Geoderma*. 2018;318:78-87. <https://doi.org/10.1016/j.geoderma.2017.11.042>
- Wadell H. Sphericity and roundness of rock particles. *J Geol*. 1933;41:310-31. <https://doi.org/10.1086/624040>
- Wardak DLR, Padia FN, Heer MI, Sturrock CJ, Mooney SJ. Zero tillage has important consequences for soil pore architecture and hydraulic transport: A review. *Geoderma*. 2022;422:115927. <https://doi.org/10.1016/j.geoderma.2022.115927>
- Ye C, Sun H, Wang H, Zhang M, Huang Z, Niu F. Microstructure properties of soft soils under marine, interactive marine, and river-lake facies sedimentary environments. *Appl Ocean Res*. 2023;130:103445. <https://doi.org/10.1016/j.apor.2022.103445>
- Yudina A, Kuzyakov Y. Dual nature of soil structure: The unity of aggregates and pores. *Geoderma*. 2023;434:116478. <https://doi.org/10.1016/j.geoderma.2023.116478>